



Cite this: *Phys. Chem. Chem. Phys.*, 2017, **19**, 11748

Received 17th February 2017,
Accepted 19th April 2017

DOI: 10.1039/c7cp01074e

rsc.li/pccp

The weakly coordinating binary macropolyhedral anion *closo,closo*-[B₂₁H₁₈][−] (B21; D_{3h} symmetry) has been synthesized using a simplified strategy compared to that in the literature. While gas-phase complexes of B21 with β- and γ-cyclodextrin (CD) were detected using ESI FT-ICR spectrometric measurements, α-CD did not bind to the B21 guest. This spectroscopic evidence has been interpreted using quantum-chemical computations, showing that β- and γ-CD are able to interact with B21 due to their larger cavities, in contrast to the smaller α-CD. The hydridic B–H vectors of the B21 anion interact with K⁺ counterions and, via dihydrogen bonding, also with the partially positively charged hydrogens of the CD sugar units in the modeled β- and γ-CD complexes. In summary, it has been shown by combined spectrometric/computational analysis that macropolyhedral boron hydride anions with two counterions can form stable complexes with β- and γ-CD in the gas phase, offering a new perspective for the future investigation of this remarkable anion in the areas of supramolecular and medicinal chemistries.

Introduction

The icosahedron is the most symmetrical way to arrange twelve atoms into a polyhedral cluster. It is the quintessential structural

motif in boron hydride cluster chemistry, represented by the *closo*-[B₁₂H₁₂]^{2−} dianion, which has I_h point-group symmetry. While parent boron hydrides have a tendency to fuse together, this happens not through a single shared boron atom, but rather requires at least one joint B–B vector.¹ In the case of the joining of two *closo*-[B₁₂H₁₂]^{2−} cages, three vertices need to be shared.² On that basis, *closo,closo*-[B₂₁H₁₈][−] (abbreviated as B21 in this study) is formed by the oxidative coupling of two *closo*-[B₁₀H₁₀]^{2−} clusters. The resulting *closo,closo*-[B₂₀H₁₈]^{2−} macropolyhedral anion is isomerized, which is followed by the insertion of an additional boron vertex by heating with BH₃·NEt₃.³ The B21 anion adopts overall D_{3h} symmetry, indicative of four symmetrically unique boron environments instead of one in *closo*-[B₁₂H₁₂]^{2−} (Fig. 1).

Boron clusters form a number of unique types of noncovalent interactions,⁴ of which dihydrogen bonding⁵ and B–H···cation interactions are important for this study. Both interactions are based on the fact that boron-bound hydrogens are slightly negatively charged due to the lower electronegativity of boron as compared to hydrogen. This is evident from the calculated

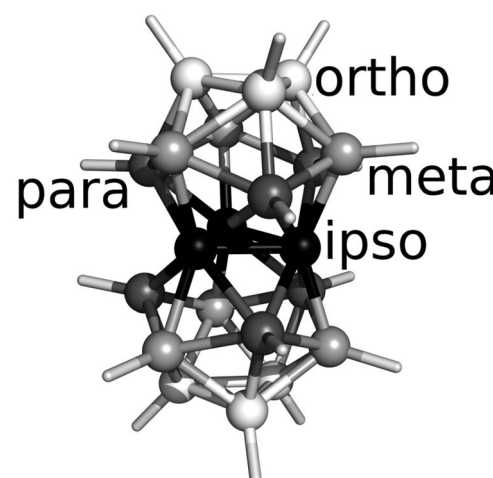


Fig. 1 A molecular diagram of *closo,closo*-[B₂₁H₁₈][−] with D_{3h} symmetry that distinguishes between individual types of boron atoms.



electrostatic potential (ESP) or partial atomic charges obtained by the restrained fit to the electrostatic potential (RESP) methodology.⁶ These two types of interaction (B–H···cation interactions⁷ and dihydrogen bonding⁸) have been found to be crucial for the binding of boron-cage-containing inhibitors to protein receptors. Host–guest chemistry presents a broad field of supramolecular chemistry, that is based on the specific non-covalent recognition of inorganic ions or small-molecule organic guests by macrocyclic organic hosts. Typically, cationic or neutral guests are encapsulated into the cavity of neutral macrocyclic hosts. Cyclodextrin (CD) molecules, very well-known macrocyclic hosts, have three major forms differing in the number of glucose ring molecules: α -CD contains six, β -CD seven and γ -CD eight units. CDs are able to encapsulate in their cavities a wide range of hydrophobic organic guests; in contrast, only a few heteroborane-based guests have been reported.⁹

The complexation of boron cluster anions with hosts has been observed in solution in several examples. In each of the known complexes the anions have adopted the icosahedral structural motif.¹⁰ To our knowledge, reported gas-phase complexes with the same cage architecture are exceptional.¹¹ The study mentioned in ref. 11a reports very strong intrinsic intermolecular interactions of *closo*-[B₁₂X₁₂]²⁻ (X = H, F, Cl, Br and I) with several neutral organic receptors, where these dianionic halogenated *closo*-dodecaborates displayed selectivity for the large hosts with deep hydrophobic polarizable pockets, such as in the case of tetrathiafulvalene-based hosts or spherical cavities in the case of CDs. It is the *closo*-[B₁₂F₁₂]²⁻ anion that strongly interacts with β -CD as reported in ref. 11a. The formation of these charged complexes was proven by means of electrospray ionization mass spectrometry (ESI-MS), which is a powerful tool to study the stoichiometry and interactions of supramolecular assemblies in the gas phase.^{12–16} Postulated weak gas-phase basicities (GB) of these dianions served as an alternative explanation for the stability of these gas-phase complexes.

It is important to mention that (also due to its complicated synthesis³) no parent *macropolyhedral* borate has been found to interact with any organic molecule. We have therefore undertaken investigations aimed at testing the possibilities of the mutual interaction of purely organic and purely inorganic systems in the gas phase, the inorganic species being a unique

joint-icosahedral boron hydride. The results are important for the understanding of macropolyhedral boron cluster affinity since this cluster is relatively inert to conventional substitution reactions, and because its structure differs from its geometrical building block, the *closo*-[B₁₂H₁₂]²⁻ dianion.

Results and discussion

Simplified synthesis of B21

We based our synthesis on the synthetic procedure of **B21** reported in ref. 3. However, we have improved one step in this reaction pathway; namely the rearrangement of *trans*-[B₂₀H₁₈]²⁻ upon protonation in anhydrous HF, which provides the face-shared *fac*-[B₂₀H₁₈]²⁻. In order to avoid this time-consuming operation, we have proposed a simple step based on the reaction of the triethylammonium salt of *trans*-[B₂₀H₁₈]²⁻ with BF₃·Et₂O in the presence of dioxane. Indeed, this yields the *fac*-[B₂₀H₁₈]²⁻ isomer in the form of its trimethyl ammonium salt, which would otherwise be difficult to obtain, in 80% yield based on the starting *trans* isomer.

Mass spectrometry

Although several ESI detection conditions were examined by optimizing the corresponding FT-ICR parameters, the binary (**B21** + CD) complexes were not detected using mass spectrometry. In the negative mode of the ESI FT-ICR spectrum (Fig. S1 (ESI[†]); *m/z* range <300), we found isotopic mass distribution of a very high-intensity peak corresponding to the singly-charged anion **B21**. In the positive mode, *m/z* values higher than 1400 (for the β -CD case) or 1600 (for the γ -CD case) were identified, with mono-charged cationic complexes of the $[\beta\text{-CD} + \text{KB21} + \text{K}]^+$ and $[\gamma\text{-CD} + \text{KB21} + \text{K}]^+$ types being formed. Each of them is depicted with its corresponding isotopic mass distributions in Fig. 2.

Computational section

Electronic properties of B21. The hitherto unknown electronic properties of isolated **B21** were studied initially using QM methods. The computed electrostatic potential (ESP) surface of **B21** indicates that the negative charge is distributed over the whole molecule (see Fig. 3). Consequently, all BH vertices should possess similar

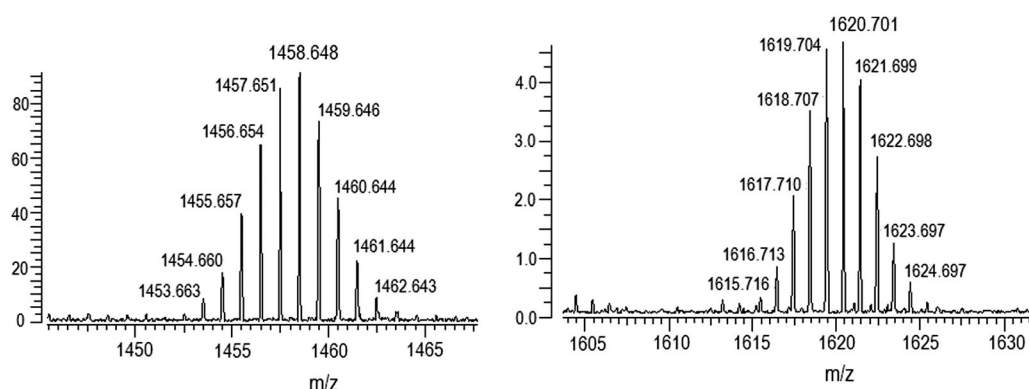


Fig. 2 The ESI FT-ICR spectra, in the positive mode, showing the isotopic mass distribution of cationic complexes formed by **KB21** with β -CD (left, the range of $1445 < m/z < 1470$) and γ -CD (right, the range of $1600 < m/z < 1635$).



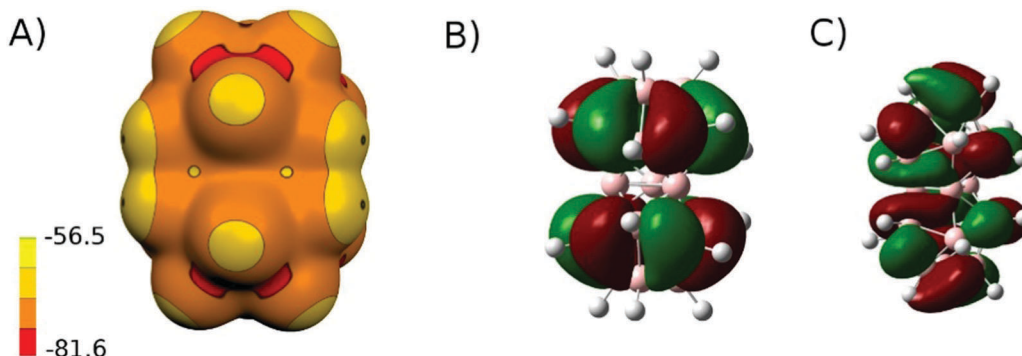


Fig. 3 The electrostatic potential (ESP) surface on 0.001 a.u. computed at the HF/6-31G* level (A). The ESP color range in kcal mol^{-1} . The HOMO (B) and LUMO (C) of **B21** were derived at the same level of theory.

chemical properties. As indicated by the HOMO of **B21**, attack by H^+ can occur close to each of the *ortho*, *meta*, and *para* BH vertices (cf. Fig. 1). Indeed, three structures of **HB21** differed in the positions of H^+ in relation to these three kinds of BH vertices; all were quite similar in energy. The “*meta*”-**HB21** isomer was about 2.3 kcal mol^{-1} less stable than “*para*”-**HB21**, *i.e.* its population at 295 K should be below 2%. On the other hand, the energetic difference between “*ortho*”-**HB21** and “*para*”-**HB21** was only 0.6 kcal mol^{-1} , with the structure in which the proton was close to the *para* boron atom computed as the most stable one. This would lead to a mixture containing 75% “*para*”-**HB21**. The structure with the extra H atom bonded to an *ipso*-boron atom was a first-order stationary point. From these calculations the gas-phase basicity¹⁷ (GB) of **B21** was computed to be 233.1 kcal mol^{-1} , a value very close to the experimentally determined GB for histidine (232.9 kcal mol^{-1}).¹⁸ The gas-phase acidity of water is reported to be 158.3 kcal mol^{-1} .¹⁹ In order to compare GB of **B21** with that of other boron clusters forming stable complexes with CDs in the gas phase, we also computed GB values for *closo*-[B₁₂H₁₂]²⁻ and *closo*-[B₁₂F₁₂]²⁻. The obtained GB values were 355.5 and 313.7 kcal mol^{-1} , respectively. **B21** is, therefore, a considerably weaker base in the gas phase than the icosahedral boron clusters. The weak GB enables *closo*-[B₁₂F₁₂]²⁻ to form stable binary dianionic complex with β -CD,^{11a} although no structure of this complex has yet been reported.

Complexes. Initial energy scans were performed for the [α -CD + **B21**], [β -CD + **B21**] and [γ -CD + **B21**] binary complexes, revealing that α -CD could not encapsulate **B21** due to the small size of the host (the energy minimum was found at a distance of 5.5 Å; Fig. 4). As a consequence, α -CD was disregarded from further consideration. The [β -CD + **B21**] and [γ -CD + **B21**] complexes exhibited a fully encapsulated minimum (z-distances of 2.0 and 1.0 Å, respectively), which is consistent with experimentally observed bound complexes.

In order to understand the complex formation of [β -CD + **B21** + 2K⁺] and [γ -CD + **B21** + 2K⁺] complexes, we analyzed not only the total interaction energies of the quaternary complexes but also all other possible pairwise interactions that can occur within the studied complexes. The obtained interaction energies are summarized in Table S1 (ESI[†]).

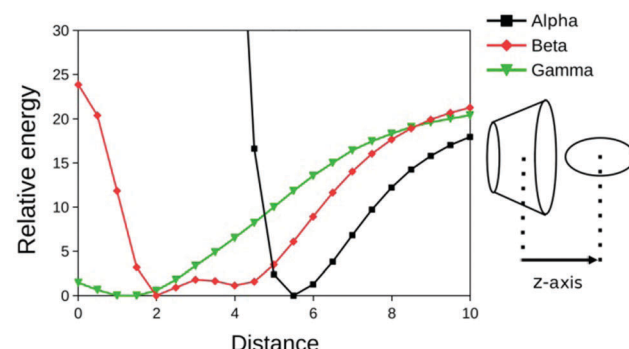


Fig. 4 DFT-D3/TPSS/TZVPP potential energy scans. Relative energy in kcal mol^{-1} and distance in Å.

Complexes of **B21 with K⁺.** The highly symmetrical structure of **B21** resulted in only four binding modes for K⁺. Fig. S2 (ESI[†]) shows the three most favorable positions according to the computations performed. The K⁺ ion interacts with four BH vertices of **B21** (two *meta* and two *para*), and the affinity of **B21** to a single K⁺ ion is directly proportional to the number of donor hydrogens. When two K⁺ ions interact with **B21**, the mutual positions of the K⁺ ions are more important than the number of hydrogen donors. The most stable arrangement occurs when the K⁺ ions are located on opposite sites, *i.e.* interacting with (a) three *ortho* BH vertices or (b) two *meta* and two *para* BH vertices (see Fig. S3, ESI[†]).

Complexes of β -, γ -CD with K⁺. The most stable binding position of K⁺ ion to the host molecules was dictated by the smaller openings of the CD molecules (see Fig. S4, ESI[†]). The K⁺ ion caused significant ring deformations for both β - and γ -CD.

Complexes of β -, γ -CD with B21. The structures obtained show that the chance of the guest molecule penetrating the cavity is proportional to the host molecule size (Fig S5, ESI[†]). γ -CD with its larger cavity is a more favorable host than β -CD (Fig. S5, ESI[†]). The interaction energies for the [β -CD + **B21**] and [γ -CD + **B21**] complexes were computed to be -24.8 and -31.0 kcal mol^{-1} , respectively. Although, the interaction energies of the binary complexes are highly negative, and the GB of **B21** is very low, the



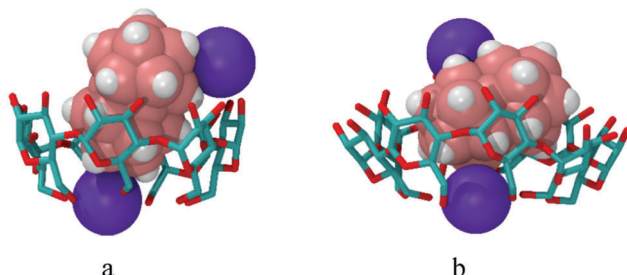


Fig. 5 The most stable computed structures of the (a) $[\beta\text{-CD} + \mathbf{B21} + 2\mathbf{K}]^+$ and (b) $[\gamma\text{-CD} + \mathbf{B21} + 2\mathbf{K}]^+$ complexes.

binary complexes were not experimentally observed under the conditions employed.

*Quaternary complexes of β -, γ -CD with **B21** and $2\mathbf{K}^+$.* The most stable $[\beta\text{-CD} + \mathbf{KB21} + \mathbf{K}]^+$ and $[\gamma\text{-CD} + \mathbf{KB21} + \mathbf{K}]^+$ complexes that are predicted by calculations are shown in Fig. 5. Armed with the knowledge of the pairwise interactions described above, we computed interaction energies according to eqn (1):

$$\Delta E = E_{(\text{total complex})} - E_{(\text{host} + \mathbf{K}^+)} - E_{(\mathbf{B21} + \mathbf{K})} \quad (1)$$

The \mathbf{K}^+ ions were placed in the small openings of the guest molecules and interacted with both O atoms of the host and H atoms of the guest molecules. They functioned as a bridge and reduced the host deformations.

It is quite apparent that the BH vertices of **B21** are of hydridic nature. The hydrogen atoms of **B21** form short contacts, *i.e.* less than 240 pm (the sum of the van der Waals radii of two hydrogens), with the partially positively charged hydrogens bonded to carbon or oxygen atoms of the sugar units. The $[\beta\text{-CD} + \mathbf{B21} + 2\mathbf{K}]^+$ complex exhibited six (prevailingly *meta* BH) vertices, with the distances ranging from 184 to 219 pm, whereas the $[\gamma\text{-CD} + \mathbf{B21} + 2\mathbf{K}]^+$ complex had seven vertices (of all kinds) and the distances ranged from 198 to 237 pm. In both cases the shortest dihydrogen bond was a result of the participation of a polar hydroxyl group. **B21** penetrated the cavity of β -CD almost parallel to the z axis (see Fig. 5a) in the $[\beta\text{-CD} + \mathbf{B21} + 2\mathbf{K}]^+$ complex. Furthermore, the conformation of $[\beta\text{-CD} + \mathbf{K}]^+$ in the $[\beta\text{-CD} + \mathbf{B21} + 2\mathbf{K}]^+$ complex is 27.2 kcal mol⁻¹ less stable than the optimal geometry of isolated $[\beta\text{-CD} + \mathbf{K}]^+$, which considerably affects the resulting interaction energy. In the $[\gamma\text{-CD} + \mathbf{B21} + 2\mathbf{K}]^+$ complex, on the other hand, **B21** binds γ -CD in a position perpendicular to the z axis (see Fig. 5b). The weaker interactions (*e.g.* longer dihydrogen bonds, see above) in the $[\gamma\text{-CD} + \mathbf{B21} + 2\mathbf{K}]^+$ complex were compensated by the smaller penalty for $[\gamma\text{-CD} + \mathbf{K}]^+$ deformation (an energy penalty of 14.3 kcal mol⁻¹). Consequently, the computed total interaction energies of the $[\beta\text{-CD} + \mathbf{B21} + 2\mathbf{K}]^+$ and $[\gamma\text{-CD} + \mathbf{B21} + 2\mathbf{K}]^+$ complexes (as provided by eqn (1), *i.e.* **KB21** with $[\mathbf{CD} + \mathbf{K}]^+$) were nearly identical (-51.8 and -51.1 kcal mol⁻¹, respectively) despite differences in the **B21** binding modes to β - and γ -CDs in the quaternary complexes. Note also that outer interaction of **B21** with β -CD and γ -CD would have been disfavored since the contact surface area would be considerably reduced.

Conclusions

The synthesis of **B21** has been improved by simplifying the most complicated rearrangement in the synthetic procedure. This allowed **B21** to be synthesized more quickly and in higher yield than previously. **B21** was found to be inert to various attempts to obtain mono-substituted **B21**. With the exception of $\text{B}_{\text{ipso}}\text{-B}_{\text{ipso}}$ vectors, all the remaining B-B separations contribute to the LUMO, which also features participation of the terminal hydrogens. It is possible that nucleophilic attacks (*e.g.* with OH^- or halogenide anions) occur at these B-B-H sites and no geometrical preference can be determined from the LUMO. This might account for the fact that all synthetic efforts to prepare mono-substituted **B21** resulted in the mixtures of differently substituted derivatives of **B21**.

Despite the low chemical reactivity of **B21**, we observed gas-phase interactions of **B21** with β - and γ -CD. These interactions were examined by ESI FT-ICR spectrometric measurements. In contrast to both larger CDs, α -CD did not bind the anion, which was explained by its spatial requirements. The structures of both β - and γ -CD complexes were determined using QM calculations. Hydridic B-H vertices of the anion interact both with the partially positively charged hydrogens of the sugar units *via* dihydrogen bonding and with potassium counterions through B-H · · cation interactions in the computed structures of the complexes. The observed interactions of the anion under investigation give hope to the tantalizing possibility of promising interactions with biomolecules. Having knowledge of these kinds of interactions is of great importance, in particular with the precedence of the ability of joint icosahedra to inhibit biologically relevant targets.⁴

Acknowledgements

This work was supported by research project RVO 61388963 of the Czech Academy of Sciences. We acknowledge the financial support of the Czech Science Foundation (SME, ML, JF, PH: P208/12/G016 and DH 15-0556775). This work was supported by the Ministry of Education, Youth and Sports from the Large Infrastructures for Research, Experimental Development and Innovations project “IT4Innovations National Supercomputing Center – LM2015070” as well as from project LO1305 (PH).

References

- Such a common edge is associated with both isomers of $\text{B}_{18}\text{H}_{22}$ – see *e.g.* M. G. S. Londenborough, D. Hnyk, J. Bould, L. Serrano-Andrés, V. Sauri, J. M. Oliva, P. Kubát, T. Polívka and K. Lang, *Inorg. Chem.*, 2012, **51**, 1471–1479 and the references therein.
- It is possible to join two $\text{B}_{12}\text{H}_{12}^{2-}$ icosahedra through four joint vertices like in the case of $\text{B}_{20}\text{H}_{16}$ – see D. Hnyk, J. Holub, T. Jelinek, J. Macháček and M. G. S. Londenborough, *Collect. Czech. Chem. Commun.*, 2010, **75**, 1115–1123 and the references therein.



3 E. Bernhardt, D. J. Brauer, M. Finze and H. Willner, *Angew. Chem., Int. Ed.*, 2007, **46**, 2927–2930.

4 R. Sedlák, J. Fanfrlík, A. Pecina, D. Hnyk, P. Hobza and M. Lepšík, *Boron – the Fifth Element, Challenges and Advances in Computational Chemistry and Physics*, ed. D. Hnyk and M. McKee, Springer, Heidelberg, New York, Dordrecht and London, 2015, ch. 9, vol. 20 and the references therein.

5 J. Fanfrlík, M. Lepšík, D. Hořínek, Z. Havlas and P. Hobza, *ChemPhysChem*, 2006, **7**, 1100–1105.

6 It was recently shown that the RESP methodology described in C. I. Bayly, P. Cieplak, W. D. Cornell and P. A. Kollman, *J. Phys. Chem.*, 1993, **97**, 10269–10280 represents a method of choice for heteroboranes. This is in contrast with NBO, which closely corresponds to the picture of localized bonds and lone pairs as basic units of molecular structure. This is not true for delocalized heteroboranes. More details can be found in ref. 5.

7 J. Fanfrlík, J. Brynda, J. Řezáč, P. Hobza and M. Lepšík, *J. Phys. Chem. B*, 2008, **112**, 15094–15102.

8 (a) M. Kožíšek, P. Cíglér, M. Lepšík, J. Fanfrlík, P. Řezáčová, J. Brynda, J. Pokorná, J. Plešek, B. Grüner, K. Grantz Šašková, J. Václavíková, V. Král and J. Konvalinka, *J. Med. Chem.*, 2008, **51**, 4839–4843; (b) J. Brynda, P. Mader, V. Šicha, M. Fábry, K. Poncová, M. Bakardiev, B. Grünwe, P. Cíglér and P. Řezáčová, *Angew. Chem., Int. Ed.*, 2013, **52**, 13760–13763; (c) A. Pecina, M. Lepšík, J. Řezáč, J. Brynda, P. Mader, P. Řezáčová, P. Hobza and J. Fanfrlík, *J. Phys. Chem. B*, 2013, **117**, 16096–16104.

9 K. I. Assaf, D. Gabel, W. Zimmermann and W. M. Nau, *Org. Biomol. Chem.*, 2016, **14**, 7702–7706.

10 (a) A family of *closo* dodecaborate anions of the type $[B_{12}X_{12}]^{2-}$ and $[B_{12}X_{11}Y]^{2-}$ (X = H, Cl, Br and I; Y = OH, SH, NH_3^+ and NR_3^+) was tackled, see K. I. Assaf, M. S. Ural, F. Pan, T. Georgiev, S. Simova, K. Rissanen, D. Gabel and W. M. Nau, *Angew. Chem., Int. Ed.*, 2015, **54**, 6852–6856; (b) Complexes of a neutral icosahedron with CD are reported in P. Neirynck, J. Schimer, P. Jonkheim, L.-G. Milroy, P. Cíglér and L. Brunsved, *J. Mater. Chem. B*, 2015, **3**, 539–545.

11 (a) J. Warneke, C. Jenne, J. Bernarding, V. A. Azov and M. Plaumann, *Chem. Commun.*, 2016, **52**, 6300–6303; (b) Interestingly, the same perfluorinated dodecaborate anion interacts in the gas-phase with all *cis* 1,2,3,4,5,6-hexafluorocyclohexane, see M. J. Lecours, R. A. Marta, V. Steinmetz, N. Keddie, E. Fillion, D. O'Hagan, T. B. McMahon and W. Scott Hopkins, *J. Phys. Chem. Lett.*, 2017, **8**, 109–113.

12 C. A. Schalley, *Mass Spectrom. Rev.*, 2001, **20**, 253–309.

13 J. Černochov, P. Brann, M. Rouchal, P. Kulhánek, I. Kuritka and R. Vícha, *Chem. – Eur. J.*, 2012, **18**, 13633–13637.

14 J. W. Lee, S. W. Heo, S. J. C. Lee, J. Y. Ko, H. Kim and H. I. Kim, *J. Am. Soc. Mass Spectrom.*, 2013, **24**, 21–29.

15 G. Carroy, V. Lemaury, J. De Winter, L. Isaacs, E. De Pauw, J. Cornil and P. Gerbaux, *Phys. Chem. Chem. Phys.*, 2016, **18**, 12557–12568.

16 T.-C. Lee, E. Kalenius, A. I. Lazar, K. I. Assaf, N. Kuhnert, C. H. Grün, J. Jänis, O. A. Scherman and W. M. Nau, *Nat. Chem.*, 2013, **5**, 376–382.

17 Note that the gas-phase acidity of 1-COOH-1,7-*closo*-[C₂B₁₀H₁₁] is measured to be 316.7 kcal mol⁻¹ (315.7 kJ mol⁻¹ as computed at B3LYP/6-311++G(d,p)) and reported in J. Z. Dávalos, J. González, R. Ramos, D. Hnyk, J. Holub, J. A. Santaballa, M. Canle-L. and J. M. Oliva, *J. Phys. Chem. A*, 2014, **118**, 2788 and the references therein. Note also that *closo*-[H(B₁₂F₁₂)]²⁻ act also as Brønsted acid, which precludes deprotonation of β-CD in the complex and the concept of weak GB as a driving force for the complex stability is justified, see C. Jenne, M. Kessler and J. Warneke, *Chem. – Eur. J.*, 2015, **21**, 5887–5891 and L. Lipping, I. Leito, I. Koppel, I. Krossing, D. Himmel and I. A. Koppel, *J. Phys. Chem. A*, 2015, **119**, 735–743.

18 G. Bouchoux, *Mass Spectrom. Rev.*, 2012, **31**, 391–435.

19 I. Leito, I. A. Koppel, P. Burk, S. Tamp, M. Kutsar, M. Mishima, J.-L. M. Abboud, J. Z. Dávalos, R. Herrero and R. Notario, *J. Phys. Chem. A*, 2010, **114**, 10694–10699.

